(Preprint) AAS 20-718

AERODROP: PROSPECTS AND CHALLENGES FOR CO-DELIVERY OF PROBE AND ORBITER VIA AEROCAPTURE

Samuel W. Albert[*], Robert D. Braun[†], and Hanspeter Schaub[‡]

AeroDrop is a new way to include ride-along probes or orbiters on interplanetary missions, made possible by the advent of small satellites as secondaries for space science missions combined with the maturation of aerocapture technologies. This mission architecture involves the design of a probe with the aerodynamic characteristics to reach the surface from the same entry state as the mothercraft performing aerocapture – or vice-versa. By eliminating the need for an in-space divert maneuver, AeroDrop lowers the additional risk of these secondary smallsats. This study summarizes the key prospects and challenges for the implementation of AeroDrop, including a feasibility assessment of the flight-mechanics and relevant constraints at Venus, Titan, and Neptune. The study also includes an analysis of relevant past missions and a discussion of the risk reduction by using AeroDrop instead of a propulsive divert maneuver. The most promising AeroDrop configuration is shown to be passive impactor or penetrator probes delivered on a ballistic nominal trajectory as the secondary mission to a primary orbiter delivered by a lift-modulated nominal aerocapture trajectory.

INTRODUCTION

Co-delivery of a probe and an orbiter is a powerful architecture for a variety of interplanetary missions. The Galileo and Cassini-Huygens missions are two famous examples, among many others, of this approach. Given the infrequency of major planetary science missions, it is highly desirable to maximize scientific return by gathering data from orbit as well as *in-situ* measurements from the atmosphere or surface. Though interplanetary co-delivery has already been accomplished a number of times, two recent developments have changed the landscape of this problem in a way that creates a new opportunity for planetary science missions.

The first development is the recent preponderance of small satellites, especially CubeSats, which have accounted for an increasingly large share of satellites launched each year since around 2012.[1] Technological innovations including the miniaturization of electronics and availability of commercial-off-the-shelf hardware has led to a steady increase in the capabilities possible in these small form-factors, and CubeSat missions have now moved beyond serving a primarily educational role to make numerous notable scientific contributions.[2] Many have recognized the potential application of small

[*]Graduate Student, Ann and H.J. Smead Aerospace Engineering Sciences, University of Colorado Boulder, Colorado Center for Astrodynamics Research, 3775 Discovery Drive, 429 UCB – CCAR, Boulder, CO 80303. AIAA Member.

[†]Professor Adjunct, Ann and H.J. Smead Aerospace Engineering Sciences, University of Colorado Boulder, Colorado Center for Astrodynamics Research, 3775 Discovery Drive, 429 UCB – CCAR, Boulder, CO 80303. AAS Fellow, AIAA Fellow.

[‡]Glenn L. Murphy Chair of Engineering, Ann and H.J. Smead Aerospace Engineering Sciences, University of Colorado Boulder, Colorado Center for Astrodynamics Research, 3775 Discovery Drive, 429 UCB – CCAR, Boulder, CO 80303. AAS Fellow, AIAA Fellow.

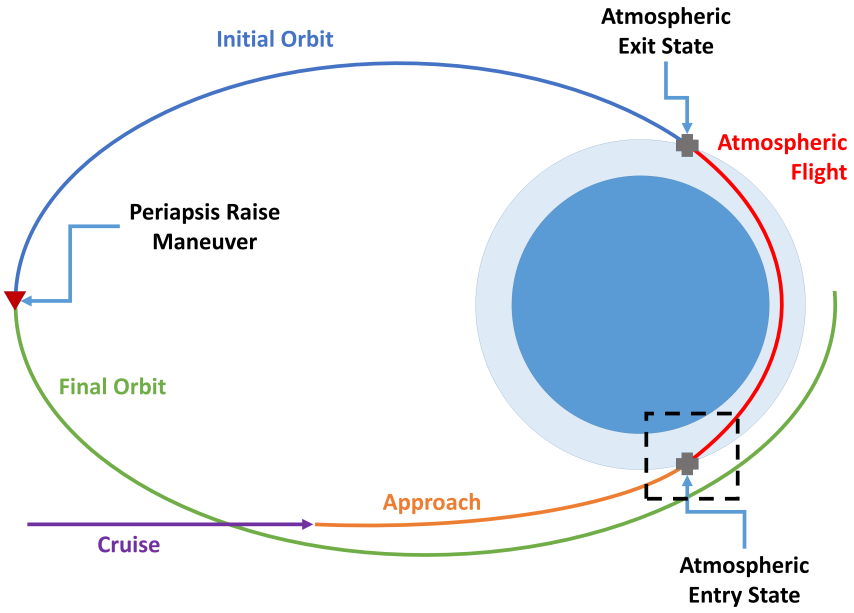

Figure 1: Diagram of the aerocapture process

satellite platforms to planetary science missions. A 2014 study sponsored by the Keck Institute for Space Studies presented space science mission concepts "uniquely enabled by the small satellite platform," and recommended including small spacecraft as secondaries on all missions beyond low Earth orbit (LEO).[3] NASA has also studied a variety of mission concepts through its Planetary Science Deep Space SmallSat Studies program.[4] In November 2018 MarCO-A and MarCO-B, the twin CubeSat communications relays accompanying the InSight Mars lander, successfully demonstrated the merit of smallsats in deep space applications.[5] Smallsat secondary spacecraft enhance planetary science missions only if the secondary mission can minimize the additional mass, risk, cost, and complexity to the primary mission.

The second recent development is the increasing technical maturity of aerocapture, the technique of flying through a planet's atmosphere in order to reduce the spacecraft's energy and capture into orbit as shown in Figure 1. This idea is far from new, having been studied for decades and proposed on a number of missions.[6,7] Aerocapture has still never been implemented in flight, though there has been some renewed interest in the area in recent years. Technology development such as the Heatshield for Extreme Entry Environment Technology (HEEET) from NASA Ames Research Center and recent work on discrete-event drag-modulation aerocapture, among others, contribute to lowering the mission risk of aerocapture.[8,9] A 2016 study at the NASA Jet Propulsion Laboratory (JPL) concluded that while aerocapture technology readiness is destination-dependent, no prior flight demonstration would be needed to implement aerocapture at Titan, Mars, and possibly Venus.[10] Some of the renewed interest in aerocapture can be attributed to a recent focus on concepts for missions to the ice giants (Uranus and Neptune) in preparation for the next Planetary Science Decadal Survey,[11] because it is these destinations where aerocapture can offer the most benefit compared to propulsive orbit insertion.[12]

The new opportunity enabled by secondary smallsats and aerocapture is AeroDrop.[13] The concept, illustrated in Figure 2, is to design a probe and an orbiter to reach their desired final states

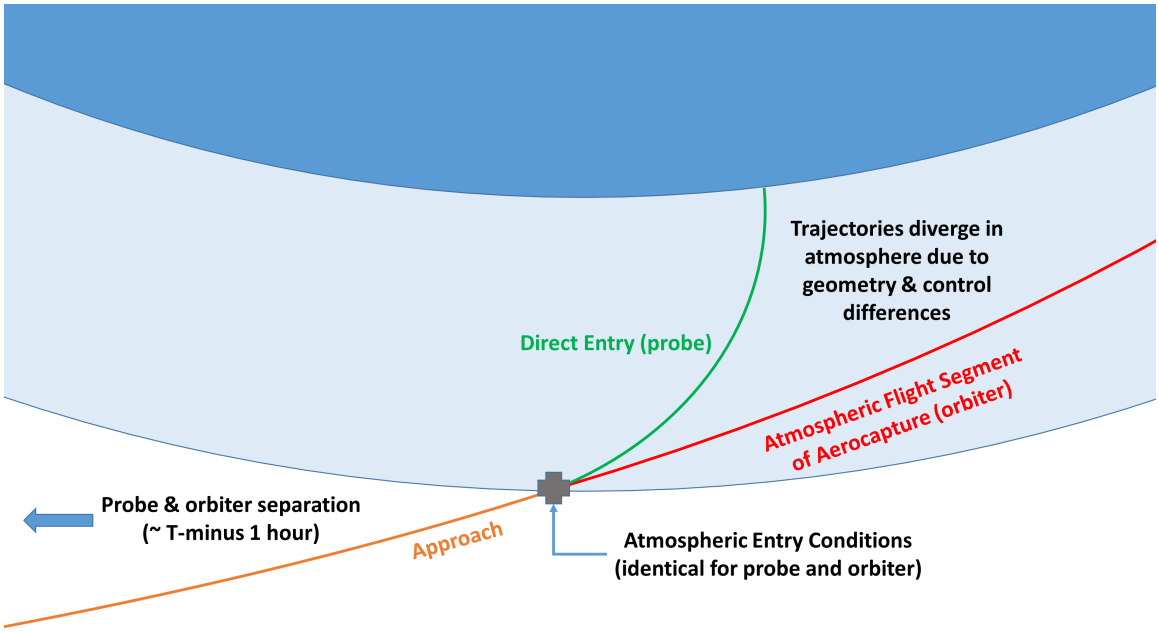

Figure 2: AeroDrop diagram, shown as a close-up view of the region in the dashed-line box in Fig. 1. Features exaggerated.

from a single approach trajectory and entry state. The two vehicles travel together during cruise until shortly before atmospheric entry, then diverge during atmospheric flight due to differences in their aerodynamic properties and control strategies. The orbiter stays higher in the atmosphere, burning off just enough energy to perform aerocapture, while the probe continues deeper into the atmosphere until either beginning a subsequent deceleration phase (i.e., deploying parachutes) or plummeting into the atmosphere or surface, as desired. Note that in this paper, "probe" is used as a catch-all term including landers, impactors, deep atmospheric probes, etc. By eliminating the need for a critical divert maneuver performed shortly before entry, AeroDrop could enable small secondary probes or landers on larger primary missions with minimal added risk and complexity. For example, a satellite using lift-modulated aerocapture to reach Mars orbit could release several small probes that follow ballistic trajectories down to the surface. In general AeroDrop can apply to missions with multiple primary or secondary spacecraft, but for simplicity this paper proceeds assuming only one probe and one orbiter.

The central purpose of this paper is to examine at a higher level the key prospects and challenges of AeroDrop; that is, to consider the potential benefits of AeroDrop to a wide range of mission scenarios as well as the biggest issues that would stand in the way of implementation. The reduced risk of AeroDrop is discussed in greater detail, and the study also includes an analysis of the applicability of AeroDrop to a number of previous real and proposed probe/orbiter missions. Peak heat-rate and integrated heat load constraints are added to the feasibility assessment results. Finally, this study expands the previous feasibility assessment to include a broader range of scenarios, including missions to Venus, Titan, and Neptune.

PROSPECTS

Advantages of AeroDrop

The key advantage of AeroDrop is that it lowers the additional mass, risk, and complexity (and therefore also cost) to the primary mission when compared to alternative co-delivery mission architectures. The risk of some of these architectures is compared to AeroDrop here, and the subsequent section discusses several specific mission concepts.

The primary and secondary spacecraft share a cruise stage. The simplest co-delivery architecture would be to handle the primary and secondary missions entirely separately starting from the time they leave Earth orbit. This without a doubt is the least imposing on the primary mission but also requires an independent secondary mission. One of the major benefits AeroDrop has over this architecture is that it allows the primary and secondary missions to share a cruise stage. This can provide the secondary spacecraft with hardware necessary for interplanetary cruise such as: solar arrays* and batteries for power, propellant and thrusters for trajectory correction maneuvers (TCMs) and attitude control, communications equipment, and thermal control systems. Furthermore, the secondary spacecraft does not impose any additional load on the operations personnel and ground assets dedicated to navigating the spacecraft to its destination. Importantly, these ground assets include the NASA Deep Space Network (DSN), and not taking any DSN time from the primary spacecraft or other ongoing missions is a selling point for the secondary mission.

The probe does not require in-space propulsion. For a primary and secondary spacecraft sharing a cruise stage, one delivery option is to carry the probe into orbit with the orbiter. A major advantage of this approach is that the orbiter can image the surface and a landing site can be selected for the probe with better knowledge of the accessible terrain. However, this architecture requires a deorbit maneuver for the probe, very likely requiring the inclusion of in-space propulsion capabilities on the probe. If the orbiter uses aerocapture to enter orbit, this architecture has additional challenges. Because the probe would still be attached to the orbiter during the atmospheric flight segment of aerocapture, both would need to share an entry system and heat shield, presenting nontrivial packaging constraints. It may be possible in some scenarios for the probe to re-use the orbiter's heat shield, but then the thermal design would have to account for heat transferred from the heatshield to the spacecraft after aerocapture. Finally, whether the orbiter uses aerocapture or propulsive orbit insertion, any propulsive maneuvers would have to be sized for the total mass of both probe and orbiter, a significant constraint if the orbiter is a small secondary mission.

If the probe is not carried into orbit with the orbiter, then in general the probe and orbiter would require different entry conditions. If the orbiter and probe share a cruise stage (and thus share an approach trajectory) but require different entry conditions, then at least one of the spacecraft will need to perform a divert maneuver before entry. The probe could divert away from the orbiter, but again this would require maneuvering capability for the probe. This in-space propulsion capability would generally not be required otherwise, so the additional mass and complexity of the propulsion system would represent a significant penalty for this architecture. In some cases the lander may have a reaction control system to control attitude during atmospheric flight, and this system could potentially perform the probe divert maneuver. However, in addition to the extra propellant mass, this approach would require the navigation hardware and software needed to compute and perform the divert maneuver and likely also a clean-up burn. This requirement would add complexity and

*Where applicable; the secondary mission could also potentially share power from a radioisotope thermal generator (RTG) unit on the primary spacecraft while attached.

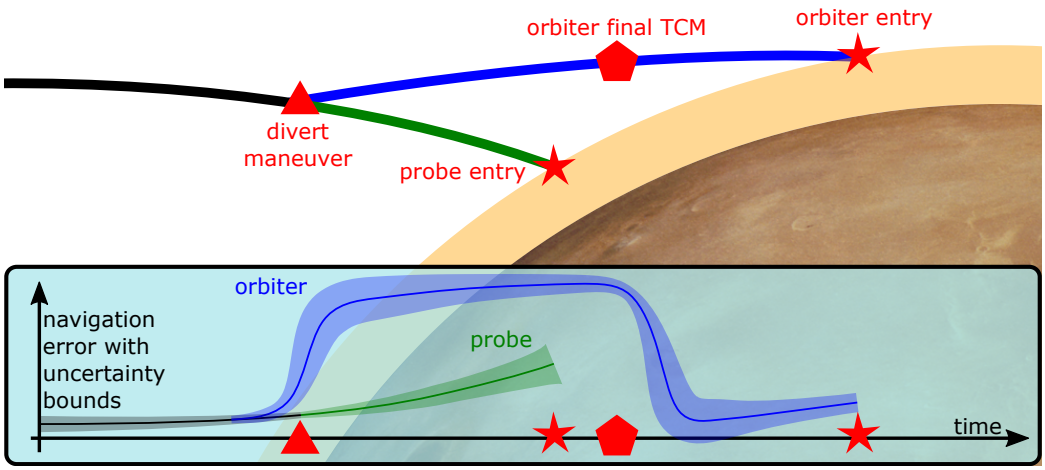

Figure 3: Illustration of orbiter-divert scenario with qualitative navigation error and uncertainty growth

cost to the probe.

The orbiter does not perform a divert maneuver. The other alternative is for the orbiter to perform a divert maneuver prior to entry. Because the orbiter already requires propulsion for the periapsis raise and later correction maneuvers (or orbit insertion, if the orbiter is not using aerocapture), this avoids any additional hardware. However, executing this divert maneuver still presents challenges, and these are illustrated in Figure 3 where the timing of the divert maneuver is shown as the triangle. In the absence of correction maneuvers, navigation error grows over time, which is why generally a TCM is scheduled for shortly arrival. The navigation uncertainty is shown as generally decreasing under the assumption that the orbiter is being tracked by the DSN and receiving regular navigation updates. Once the orbiter diverts, the probe is coasting until entry without course correction capabilities, leading to a wider range of potential entry conditions. Because the probe has no independent deep-space navigation hardware, its navigation uncertainty grows along with its error. This problem of probe navigation drives the divert maneuver timing to be as late as possible, but this causes other problems for the orbiter. Because any maneuver will be imperfectly executed, an optional clean-up TCM (shown as the pentagon) would have to be scheduled for after the divert and before entry. Collecting sufficient tracking data for a good navigation solution then computing and executing the TCM takes time, likely several days. As can be visualized from Figure 3, delaying the divert maneuver requires compressing this orbiter timeline, until at some point there is not enough time for a TCM after the divert. Because the orbiter approaches on a steep probe trajectory, failure of the divert maneuver or final TCM could result in loss of the orbiter. Finally, the later the divert is the larger the maneuver will need to be, resulting in additional propellant mass for the orbiter. Notably, these drawbacks would be eased somewhat if the orbiter had autonomous navigation capability that allowed it to generate navigation solutions and design corrective maneuvers much more quickly and without relying on signals received at Earth.

Applicability to Mission Concepts

There has been little systematic study of architectures for the co-delivery of an orbiter and a probe, but multiple missions have proposed or flown various versions of co-delivery architectures. None of these missions would make perfect candidates for AeroDrop since none use aerocapture, which has never been implemented. Nonetheless, they make instructive examples in examining the applicability of AeroDrop.

One pair of examples is the two Viking missions, each of which sent a lander and orbiter to Mars. The lander remained attached to the orbiter as it entered orbit and returned images of the Martian surface for landing site selection. After about one month in orbit, the lander deorbited itself to begin the entry, descent, and landing (EDL) sequence. The architecture choice of bringing the probe to orbit is well-suited for applications like Viking, in which more information about the atmosphere or surface at the destination is needed to ensure safe performance of the probe. Indeed, the original landing sites for both Viking 1 and Viking 2 were changed after they were declared unsafe based on orbiter photos.[14] The tradeoffs incurred by bringing the probe to orbit include the extra propellant for the orbit insertion maneuver due to the probe mass and an in-space propulsion system for the probe's deorbit maneuver. The Viking landers each carried a hydrazine rocket to execute a deorbit burn of about 180 m/s.[15] AeroDrop would not be a good solution for missions like Viking requiring reconnaissance by the orbiter in advance of probe entry. For AeroDrop, either the surface should be well-characterized in advance or the probe should be resilient to uncertainties in landing environment. Major advances since the 1970's in hypersonic aeromaneuvering, hazard avoidance, and terrain-relative navigation significantly alleviate this constraint.[16]

The Galileo and Cassini-Huygens missions were both major planetary science missions that included an atmospheric probe carried to its destination with the larger orbiter. Incredibly, both of these missions successfully implemented the orbiter divert architecture without adding any navigation or maneuvering capability to the probes, which coasted passively from release until entry. The price for this coast was larger entry dispersions, the Galileo probe coasting for nearly 150 days before entry at Jupiter with an entry flight path angle (EFPA) requirement of $\pm 1.4^\circ$ and the Huygens probe coasting for 20 days before entry at Titan with an EFPA requirement of $\pm 3^\circ$.[17,18] EFPA is defined as the angle between the velocity vector and the local horizontal, such that a velocity pointing below the horizontal has a negative EFPA. These relatively large EFPA ranges were acceptable in part because neither probe was targeting a particular landing site. The Huygens probe did survive on the surface, but was never explicitly designed as a lander.[19] For comparison, the Mars Science Laboratory (MSL) EFPA requirement pre-launch was $\pm 0.20^\circ$.[20] AeroDrop avoids this sacrifice in probe delivery accuracy by eliminating the long coast phase for the probe.

The Mars Polar Lander (MPL) carried with it the Deep Space 2 Mars Microprobes, two small penetrators aiming to search for sub-surface water and demonstrate penetrator technology for Mars. The Mars Microprobes were a true secondary mission, separating from MPL's cruise stage only 10 minutes before impact, and at just 3.6 kg each the probes were two orders of magnitude smaller than anything NASA had previously flown to other planets.[19] Although the two missions were both probes with no orbiters, the MPL-Microprobes missions make perhaps the best flown example of an AeroDrop-like architecture. AeroDrop can be applied broadly wherever the flight mechanics are feasible, but it is primarily useful as a non-intrusive way to include a small secondary opportunity with a larger mission. AeroDrop relies on tuning the ballistic coefficient (BC or β) of the secondary vehicle to reach the desired final state given the expected entry conditions, a reversal of the normal process. The BC is effectively the ratio of inertial forces to aerodynamic forces, and is defined in

Eq. (1) where m is spacecraft mass, C_D is drag coefficient, and A is reference area. The smaller the vehicle is, the less mass or area it takes to effect large changes in the BC. As an example, if the Mars Microprobes had been carried to Mars by an orbiter performing aerocapture instead of by a lander then the EFPA would have been shallower. If necessary, the Microprobes could accommodate this by enlarging the heatshield area without changing the probe mass, thus lowering the BC in order to reach the surface from a shallower entry. This relatively small change in total launch volume would enable the ride-along probes without affecting the design for the primary orbiter. Unfortunately, the failure of both MPL and the Mars Microprobes scrapped plans for later Mars Surveyor landers and secondary Mars Micromissions that would have accompanied them.[19]

$$\beta = \frac{m}{C_D A} \tag{1}$$

The Mars Cube One (MarCO) CubeSats are also a good secondary mission example, but in a different way than the Mars Microprobes. The purpose of the twin spacecraft was to provide near-real-time telemetry data relay to Earth from the InSight Mars lander during its EDL sequence, dubbed the "carry your own relay" architecture.[5] The CubeSats were not on the critical path for InSight's science mission or operational success, and were much smaller (and cheaper) than the lander. However, rather than carrying out a small independent mission like the Microprobes, MarCO provided operational support for the primary mission. This kind of collaborative secondary mission generally, and the carry your own relay architecture specifically, has broad application. Another example is the Russian Mars 96 mission, which included an orbiter, two small landers to be released a few days before entry, and two penetrators to be released from orbit, but unfortunately failed in Earth orbit.[21] The THOR Mars Impactor Mission and ARES aerial platform mission also proposed an orbiter and flyby spacecraft, respectively, to support their primary science missions on the planet.[22,23]

AeroDrop could enhance these mission architectures in a number of ways. For MarCO, the independent navigation of the two CubeSats to Mars was a significant challenge, and also took DSN time away from the primary mission.[24] These issues would be addressed by sharing a cruise stage with InSight. A current-day revisit of the Mars 96, THOR, and ARES missions could shrink the size and cost of the support orbiters using modern smallsat technologies, such as the deployable high-gain reflectarray antenna designed for MarCO.[25] Finally, the support orbiter could use aerocapture to reach orbit, which in general requires less mass than a propulsive orbit insertion,[12] thus enabling a longer scientific or operational mission than a flyby support craft like MarCO. Implementing aerocapture on a smallsat platform would be a significant advancement, but smallsat aerocapture using drag-modulation flight control has recently been studied in detail for both an Earth flight test and planetary exploration missions.[26,27]

CHALLENGES

The central challenge to implementing AeroDrop is the feasibility from a flight mechanics perspective. That is, for AeroDrop to work, both a probe and an orbiter must be able to reach their desired final states from the same entry conditions. Consider a simplified example of a primary orbiter mission using aerocapture. The science objectives drive the design of the spacecraft and desired orbit, then an aeroshell is designed to protect the vehicle during atmospheric flight. The entry velocity given by the interplanetary trajectory and the BC determined by the vehicle design will dictate some target EFPA for the orbiter to begin aerocapture. Then, a secondary probe can be designed to have a BC that will result in a lander trajectory for that same EFPA and entry velocity. The

capabilities of this probe are then designed within the constraints of the required BC. One or both of these vehicles may also make use of lift- or drag-modulation to bias their nominal trajectories and accommodate uncertainties in the atmosphere and entry state. The next section quantifies these flight mechanics trades to identify regions of feasibility for AeroDrop. Even within these feasible regions, however, there are a number of other challenges to implementing AeroDrop.

One challenge is the separation event. The orbiter and probe must separate from each other, and possibly also from a cruise stage, shortly before entry. If the timing is too early or the ΔV imparted by separation is too large, it could alter the desired trajectory for one or both spacecraft without time to correct. If the vehicles are not separated enough, there could be a risk of recontact in the atmosphere. Finally, if the vehicles failed to cleanly separate at all, that would almost certainly result in loss of both spacecraft. This study assumes a small separation such that the vehicles do not interact in the atmosphere but have identical entry conditions, but a detailed mission study would need to carefully consider separation.

The timing and observation geometry between the orbiter and probe is another challenge. Aerocapture requires a very specific trajectory through the atmosphere, so there is little flexibility to design for observations of the probe by the orbiter. Furthermore, degradation or loss of signal for the probe or orbiter is possible due to ionization of atmospheric gases during hypersonic flight, depending on the specific vehicle, trajectory, and atmosphere. Thus, using the orbiter to relay data from the probe during EDL or immediately after landing/impact would be challenging. Uninterrupted observations of a debris plume from an impactor, for example, may not be possible with an AeroDrop configuration, although initial observation followed by repeated overflights may be.

Many AeroDrop challenges are really aerocapture challenges, one of these being packaging. Because the orbiter and probe both pass through the atmosphere with AeroDrop, any hardware not disposed of before entry must survive the hypersonic flight environment, generally requiring enclosure in an aeroshell protected by a thermal protection system (TPS). For the solar panels, radiators, and antennas of a cruise stage to be useful, however, they need access outside of the aeroshell. One solution is to bring a cruise stage just for the interplanetary phase, then dispose of it before entry. This approach is mass-redundant, however, because the orbiter still needs much of that hardware once in orbit, so a second set of solar panels, antennas, etc. inside the aeroshell would be required. The alternative is an aeroshell designed to allow external access for this hardware during cruise, possibly by being able to open and close the backshell. Depending on the destination and vehicle design, an open backshell design might be possible,[10] greatly simplifying these packaging constraints.

As with any small secondary mission, tight volume and mass constraints are a challenge for AeroDrop as well. Even with recent and ongoing advancements in miniaturized hardware for smallsats, the hardware required for aerocapture or a full EDL sequence is challenging to make small and cheap enough to be appealing as a secondary mission. As a point of rough comparison, the interplanetary smallsat aerocapture study estimates a total spacecraft mass of 68 kg,[27] whereas each MarCO spacecraft was about 14 kg.[24] The Mars Microprobes, in contrast, were only 3.6 kg.[19] Passive impact probes or penetrators as the secondary mission are excellent candidates for AeroDrop because they can avoid the additional hardware required for a soft-landing (parachutes, retrorockets, etc.).

FEASIBILITY ASSESSMENT

The purpose of this section is to understand, at a high level, the combinations of trajectories and vehicles for which AeroDrop is a possibility. A wide range of entry trajectories are simulated then classified by their final states, and a number of key constraining parameters are computed. This high-level approach is meant to demonstrate the feasibility of AeroDrop at each destination and provide a starting point for further investigation of any specific mission concept.

Methodology

Each trajectory is generated using an entry dynamics simulation tool developed for this task*. The simulation numerically propagates the three degree-of-freedom motion due to point-mass gravity, lift, and drag forces acting on the vehicle. Constant aerodynamic coefficients, constant mass, zero thrust, and axisymmetric entry vehicles are all assumed for this purpose. Eq. (2) gives the gravitational force relation, and Eqs. (3) and (4) give the magnitude of the lift and drag forces, respectively.

$$\boldsymbol{F_g} = -\frac{m\mu}{|\boldsymbol{r}|^3}\boldsymbol{r} \tag{2}$$

$$|\boldsymbol{F_L}| = \frac{1}{2}\rho|\boldsymbol{V_w}|^2 C_L A \tag{3}$$

$$|\boldsymbol{F_D}| = \frac{1}{2}\rho|\boldsymbol{V_w}|^2 C_D A \tag{4}$$

In the equations above m is the mass of the spacecraft, μ is the gravitational parameter for the central body of interest, and $\boldsymbol{r}$ is the position vector from the center of the central body to the spacecraft. Furthermore, ρ is atmospheric density, A is the reference area, C_L and C_D are the lift and drag coefficients, respectively, and $\boldsymbol{V_w}$ is the wind-relative velocity vector. The wind-relative vector is the velocity of the vehicle with respect to the air in front of it, and is distinct from the inertial velocity vector $\dot{\boldsymbol{r}} = \boldsymbol{v}$. The relation between the two velocities is given below, where $\boldsymbol{\omega} = [0, 0, \Omega]^T$ and Ω is the rotation rate of the planet/moon with respect to a planet-centered inertial frame. $\boldsymbol{W}$ is the local wind velocity, including any components due to atmospheric rotation, both of which are assumed to be negligible for the purpose of this study. In this study the terms "relative entry velocity" and "relative EFPA" refer to the magnitude and angle, respectively, when taken with respect to this $\boldsymbol{V_w}$ vector rather than the inertial velocity.

$$\boldsymbol{V_w} = \boldsymbol{v} - \boldsymbol{\omega} \times \boldsymbol{r} + \boldsymbol{W} \tag{5}$$

The drag force is always directed opposite the wind-relative velocity. The lift force direction is orthogonal to the drag and velocity directions, and rotated about the velocity vector by the bank angle. In this study only full-lift-up and full-lift-down (bank angles of 0°and 180°) orientations are considered. In a lift-up orientation the velocity vector lies in the $\boldsymbol{r} - \boldsymbol{V_w}$ plane with positive $\boldsymbol{r}$ components; for lift-down, it lies in the same plane but with negative $\boldsymbol{r}$ components. Thus, the magnitude and direction of each force is defined, and the vehicle is propagated according to Newton's Second Law, $\ddot{\boldsymbol{r}} = \sum \boldsymbol{F}/m$.

The vehicle is initialized at the atmospheric interface altitude h_{atm}, a somewhat arbitrarily defined point at which sensible atmospheric density begins. For each target destination, one representative

*https://github.com/salbert21/petunia

relative entry velocity, $V_{w,0}$, is defined. The value of these and other parameters are listed for each central body in Table 1.

Table 1: Relevant Planetary Constants

Central Body	h_{atm}, km	$V_{w,0}$, km/s	k, $\text{kg}^{0.5}/\text{m}$	atm. composition by volume
Earth	125	11	1.748×10^{-4}	79.1% N_2, 20.9% O_2 [28]
Mars	125	6	1.904×10^{-4}	2.60% N_2, 95.5% CO_2, 1.95% Ar [29]
Venus	135	11.5	1.897×10^{-4}	3.50% N_2, 96.5% CO_2 [30]
Titan	800	6	1.758×10^{-4}	97.7% N_2, 2.30% CH_4 [31]
Neptune	1000	27	7.361×10^{-5}	1.50% CH_4, 79.6% H_2, 18.9% He [32]

Profiles of atmospheric density are taken from the nominal output of the Global Reference Atmospheric Model (GRAM) for that planet/moon, then linearly interpolated with altitude. To approximately characterize the effect of density variability, results include a uniform $\pm 20\%$ uncertainty in density. The actual variability in atmospheric density is not uniform with altitude, nor is it necessarily within a 20% bound; these results are included only to show a general trend of how density variability impacts the feasibility of AeroDrop.

Several potentially constraining quantities are calculated for each trajectory, one of which is peak heat rate. Specifically, the peak convective heat flux at the stagnation point for a fully catalytic surface is estimated using the Sutton-Graves method.[28] The expression is shown in Eq. 6, where $\dot{q}_s$ is total convective heat rate at the stagnation point, p_s and h_s are the total stagnation point pressure and enthalpy respectively, R_n is the effective nose radius, h_w is the surface enthalpy, and K_{SG} is a coefficient. This expression is then converted to the more useful form shown in Eq. 7 using a few assumptions for hypersonic flow. In hypersonic flow the surface enthalpy h_w is a negligible contribution to the total value, which can then be approximated as $h_s \approx V_w^2/2$.[33] Using a Newtonian flow approximation, the pressure coefficient at the stagnation point is $C_{p,s} = 2$, and freestream pressure makes a negligible contribution, so stagnation point pressure becomes $p_s = 1/2\, C_{p,s}\rho V_w^2 + p_\infty = \rho V_w^2$.[33] The modified Sutton-Graves coefficient is then $k = K_{SG}/(2\sqrt{101325})^*$. The values used in this study for k, as well as the atmospheric compositions used to compute them, are listed in Table 1.

$$\dot{q}_s = K_{SG}\sqrt{\frac{p_s}{R_n}}(h_s - h_w) \tag{6}$$

$$\dot{q}_s = k\sqrt{\frac{\rho}{R_n}}V_w^3 \tag{7}$$

To generate approximately realistic heat-rate trends, th e nose radius of the vehicle is scaled with the BC as follows. The mass and drag coefficient are set as approximately that of MSL in every case: $m = 2920\,\text{kg}$, $C_D = 1.6$.[16] The reference area is defined as the backshell area, which is computed from β, m, and C_D using Eq. 1, and then the backshell radius R_b is computed from the area. Finally, the nose radius is computed by assuming a nose bluntness of $R_n/R_b = 1/2$, which has been the case for every Mars entry vehicle to date.[34]

The other parameters computed for each trajectory are apoapsis altitude, peak g-load, and integrated heat load. Initial apoapsis is computed using the vehicle's Keplerian state at final time, and the peak g-load is the maximum sensed acceleration shown in number of Earth g's. The total heat

*The $1/\sqrt{101325}$ factor comes out of a unit conversion from atm to Pa.

load is computed by numerically integrating the stagnation point convective heat-rate over time, and thus shares the same assumptions.

Finally, there are three types of trajectories considered in this study. For ballistic trajectories, the vehicle flies passively through the atmosphere and has a lift-to-drag ratio of $L/D = 0$. These trajectories do not imply that the vehicle would have no control authority; rather, they represent trajectories for which no lift- or drag-modulation is required to fly the nominal trajectory, so any control authority would be 100% dedicated to accommodating uncertainties. The other two types of trajectories are full-lift-up and full-lift-down, which all use a value of $L/D = 0.25$. These scenarios use 100% of their control authority (lift) to bias their nominal trajectory. In terms of final energy, all reachable trajectories for a given entry state and vehicle lie between these full-lift-up and full-lift-down bounding cases. By showing these three cases, the full set of trajectories accessible with an $L/D \leq 0.25$ are characterized for each scenario.

Results

The results at each planetary destination are summarized in Figs. 4 - 8. For each of the three trajectory types, trajectories are simulated across a grid of varying EFPA and BC. These trajectories are categorized as probes if they intersect the surface (or some minimum altitude), as orbiters if they exit the atmosphere on an elliptical orbit, or as escape if they exit on a hyperbolic orbit. For each grid, at any given BC there will be some EFPA value that delineates between orbiters and probes. These EFPA values form the black line on each plot. Similarly, if the entry velocity exceeds escape velocity, there will be an EFPA value delineating between orbiters and escape trajectories, and this is shown as the purple line. The shaded regions for each line are bounded by the values of that line when the density profile is at $\pm 20\%$ of the nominal values. Therefore, any gridpoints left of the black line are probe trajectories, any gridpoints between the lines are orbiters (aerocapture), and to the right of the purple line are escape trajectories. Contours of apoapsis altitude, peak g-load, peak heat-rate, and total heat load are then overlaid for each plot. Note that the contour values are chosen for visibility and are not necessarily evenly incremented, and that the x-axis scale varies significantly between destinations.

The interpretation of these plots is illustrated through example. By definition AeroDrop is feasible where a probe trajectory and orbiter trajectory both exist at the same EFPA for realistic BCs. Because in AeroDrop the vehicles always share an entry condition, in these plots scenarios are identified with vertical cross-sections along a single EFPA. As a simple example, a vertical line at -5.5°for the Earth-ballistic plot would pass through the middle of the black line. Here, BCs less than $75\,\mathrm{kg\,m^{-2}}$ are probes, and greater than $100\,\mathrm{kg\,m^{-2}}$ are orbiters. Thus, for 11 km/s -5.5°at Earth AeroDrop is possible using only ballistic trajectories, just by tuning the BCs of the two vehicles.

The application of lift broadens this feasible range significantly. In Fig. 4 a light blue vertical line is added at a nominal EFPA of -6.25°. On the ballistic plot the line is entirely behind the orbiters/probes cutoff, meaning all BCs in the range considered (10 - $200\,\mathrm{kg\,m^{-2}}$) result in probe trajectories. On the full-lift-up plot the line is entirely in front of the cutoff line, so all BCs result in orbiter trajectories. The initial apoapsis altitudes for these trajectories vary with BC, and are shown in the dashed blue contour lines.

For AeroDrop to be plausible, the architecture should be robust to a number of uncertainties, including navigation uncertainty. This can be described as an entry corridor, a range of possible EFPA values. In Fig. 4 the dashed light blue vertical lines represent an entry corridor for an EFPA

of $-6.25^\circ \pm 0.5^\circ$. As a result of this uncertainty the dashed lines now intersect the black cutoff lines for ballistic and lift-up trajectories, and these intersection points give the BC requirements for this scenario. For AeroDrop to be feasible even with this EFPA uncertainty the orbiter BC would need to be at least $40\,\mathrm{kg\,m^{-2}}$, and the probe coefficient no greater than $150\,\mathrm{kg\,m^{-2}}$.

These BC values might be further constrained by other requirements. Continuing the example annotated in Fig. 4, to achieve an initial apoapsis altitude of at least 150 km, the orbiter BC should be at least $70\,\mathrm{kg\,m^{-2}}$. To keep the total heat load at the stagnation point below $20\,\mathrm{kJ\,m^{-2}}$, the probe BC should be no greater than $125\,\mathrm{kg\,m^{-2}}$. Finally, note that the EFPA range still does not intersect the cutoff line on the full-lift-down plot, so any BC in range would result in a probe trajectory, although the peak g-loads are significantly higher for lift-down trajectories.

The example above demonstrates how a mission designer can choose constraints on nominal EFPA, entry corridor, apoapsis, etc. and then directly assess the feasibility of AeroDrop for that mission scenario from the plots in Figs. 4 - 8.

Discussion

The feasibility of AeroDrop at each destination depends on the specific scenario and constraints, making it hard to compare the destinations directly. One heuristic approach is to consider the EFPA range spanned by the probes/orbiters cutoff line, i.e. the difference between the transition EFPA for $\beta = 200\,\mathrm{kg\,m^{-2}}$ and for $\beta = 10\,\mathrm{kg\,m^{-2}}$. This value is about 1° at Earth, Venus, and Neptune, about 1.5° at Mars, and about 4.5° at Titan. These values reflect the entry corridor width available using two ballistic trajectories, meaning Titan is by far the most flexible for AeroDrop if no nominal lift is required. A similar heuristic parameter is the EFPA range gained from a full-lift-up trajectory, defined as the difference between the transition EFPA for $\beta = 50\,\mathrm{kg\,m^{-2}}$ with full-lift-up and for $\beta = 150\,\mathrm{kg\,m^{-2}}$. This value is about 1° for Earth, Mars, and Neptune, about 1.5° for Venus, and only about 0.5° at Titan. This reflects the fact that lift-modulation is more effective at higher entry velocities, where the control authority increases due to a larger lift magnitude. The representative entry velocity chosen for Venus is high relative to the planet's mass, and the low scale height of the Venusian atmosphere results in high densities at aerocapture altitudes. It is important to note that these benefits are directly traded-off by high g-loads, heat-rates, and heat-loads at Venus; the high entry velocity at Neptune has similar drawbacks.

There are some key limitations to the approach taken in this study. For the sake of space, only one entry velocity is considered for each destination. Different entry velocities do affect the apoapsis altitude, heat rates, and other parameters, but changes on the order of 1 km/s do not dramatically affect the feasibility of AeroDrop in general.[13] Another limitation is the bounding case approach to lift-modulation. While it is possible to use 100% of available lift to bias the nominal trajectory – Viking flew a full-lift-up trajectory with no guidance – in general some control authority must be allocated to compensate for uncertainties in EFPA, atmospheric density, vehicle parameters, etc. MSL, for example, used about 70% of its available lift to bias its nominal trajectory, reserving 30% for control authority margin.[35] The ability of the results shown here to capture these types of trajectories is limited. For example, for a lift-up trajectory at Earth, 11 km/s, EFPA of -6°, a BC of $50\,\mathrm{kg\,m^{-2}}$ results in an apoapsis altitude of about 3000 km. Intuitively, a similar trajectory that instead uses only 70% of its lift for the nominal trajectory would result in aerocapture with a lower apoapsis, but the results shown here do not quantify this idea. Nonetheless, the results shown here give bounding cases within which a vehicle could reserve some control margin for uncertainties by targeting a lower apoapsis or increasing control authority by increasing L/D.

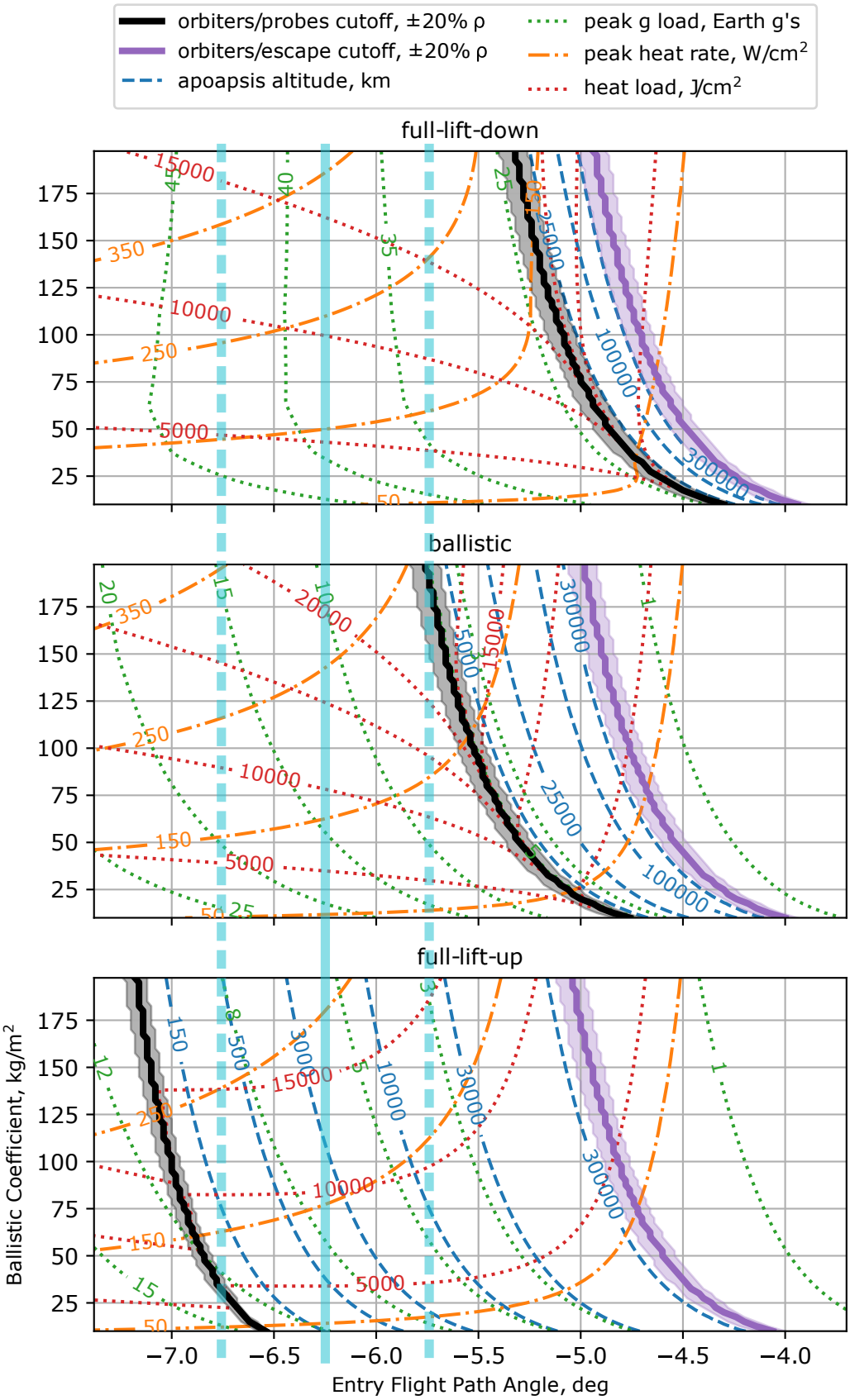

Figure 4: AeroDrop feasibility space for Earth, 11 km/s relative entry velocity, shown with example annotation

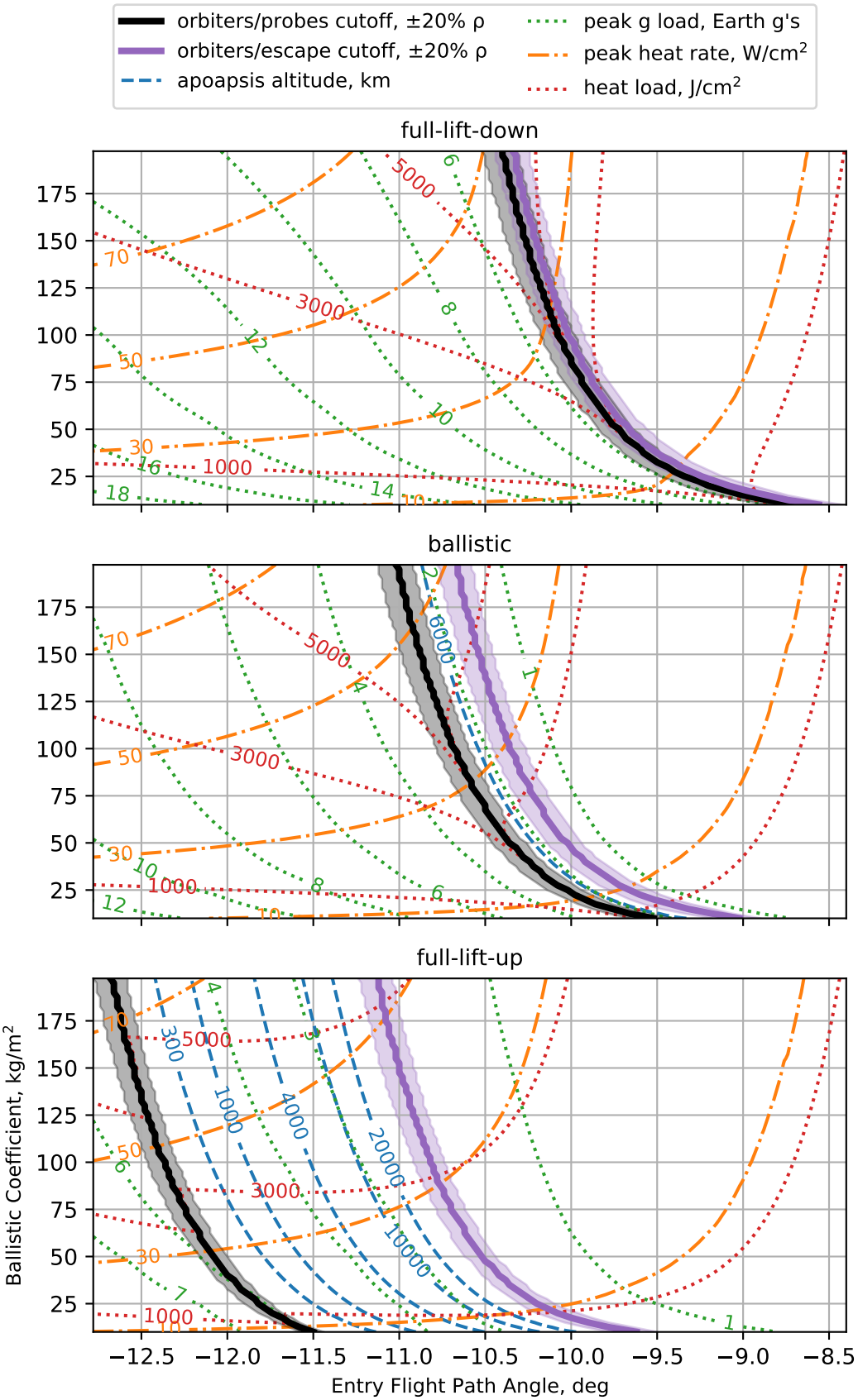

Figure 5: AeroDrop feasibility space for Mars, 6 km/s relative entry velocity

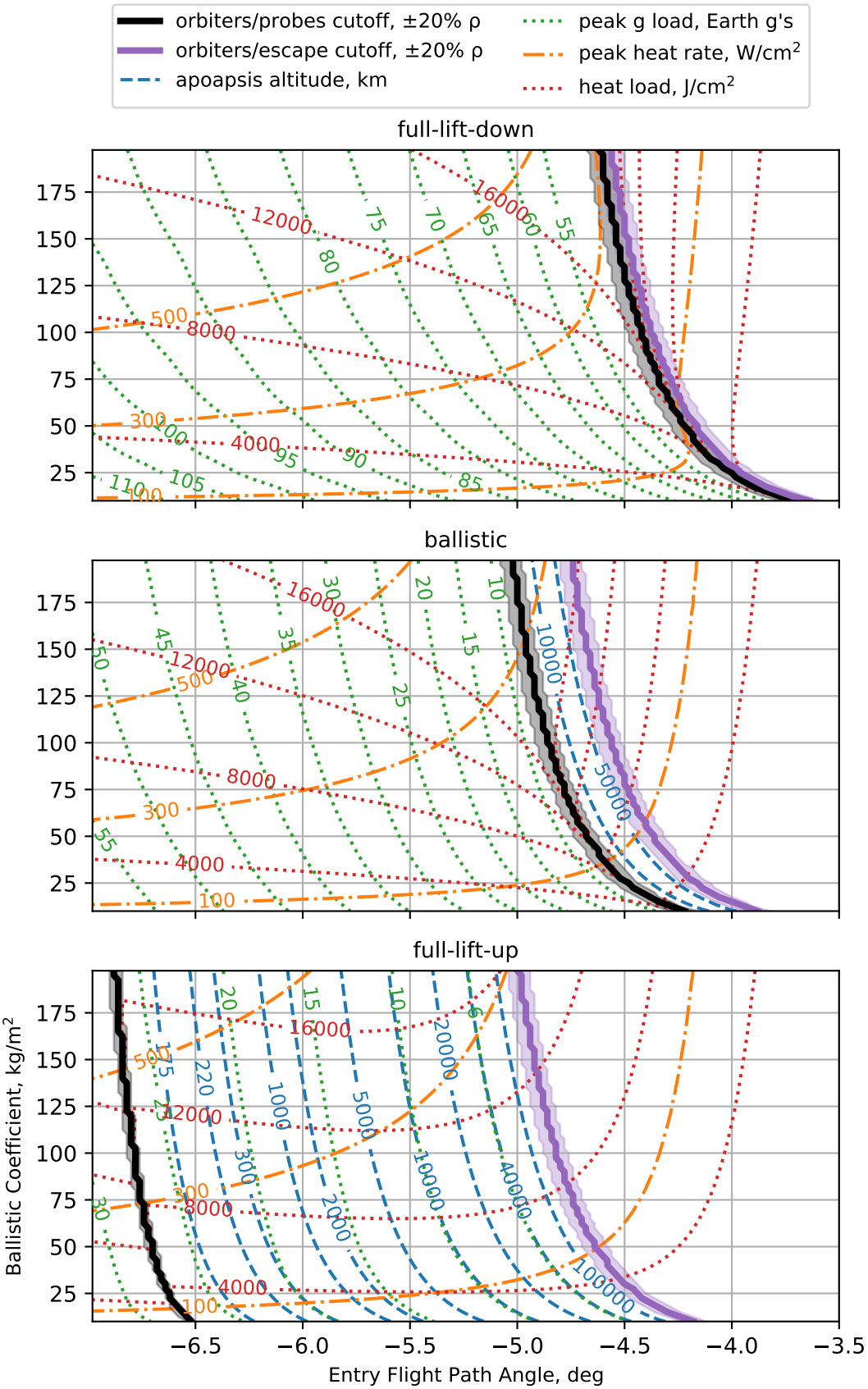

Figure 6: AeroDrop feasibility space for Venus, 11.5 km/s relative entry velocity

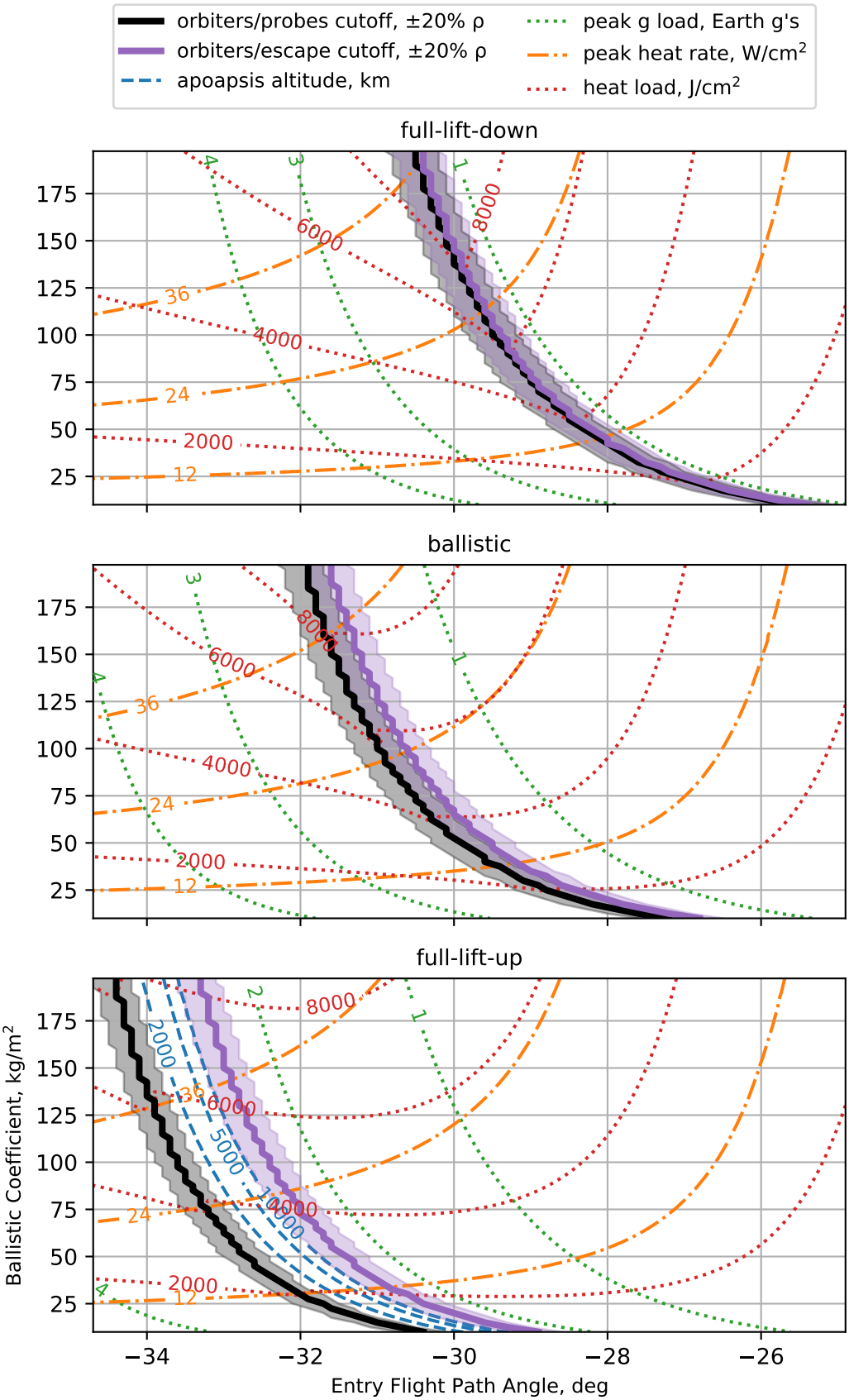

Figure 7: AeroDrop feasibility space for Titan, 6 km/s relative entry velocity

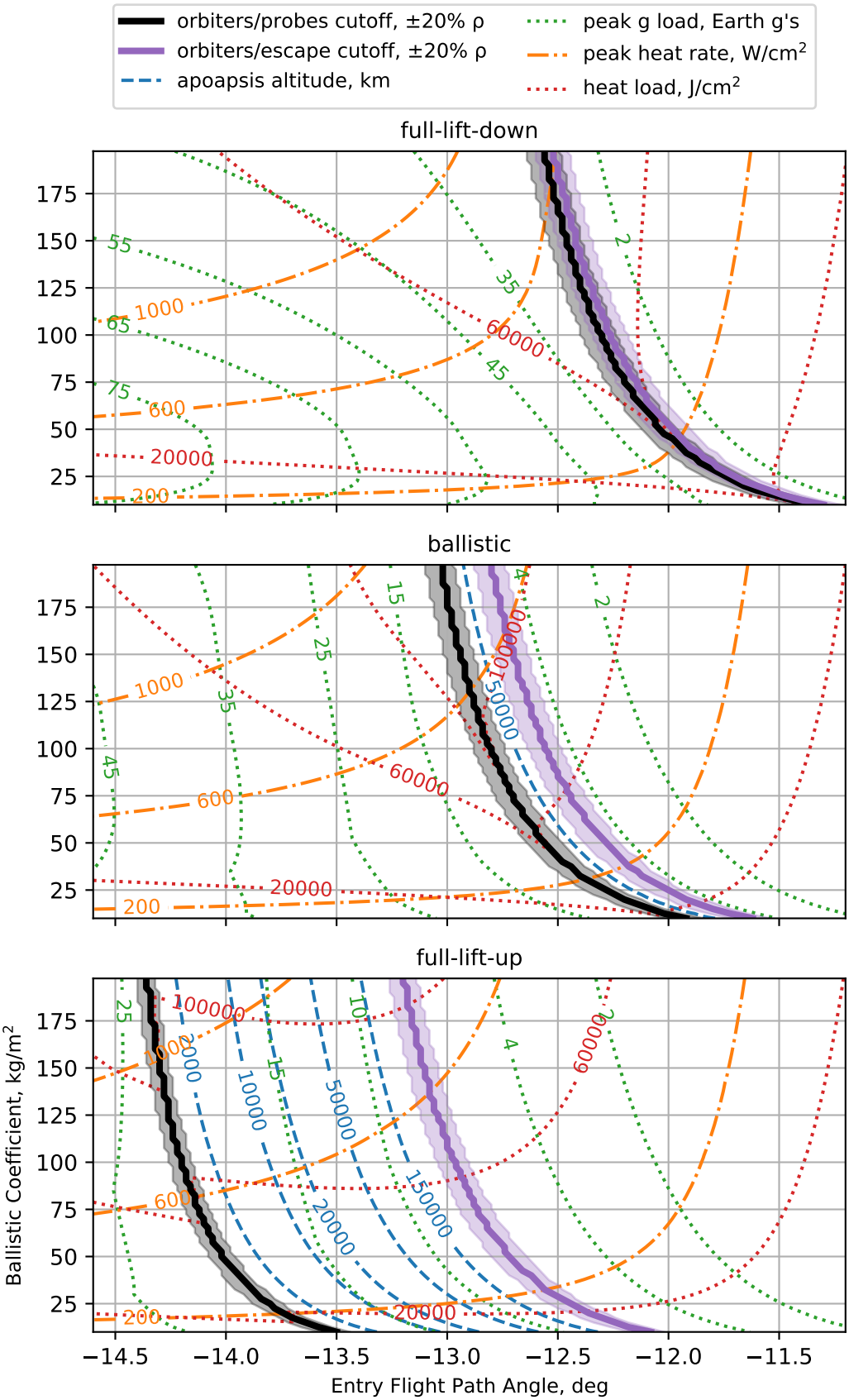

Figure 8: AeroDrop feasibility space for Neptune, 27 km/s relative entry velocity

Another aerocapture trade reflected in these results is that, in general, more is gained from the lift-up trajectories than from lift-down. From inspection of the example in Fig. 4, it is clear than one appealing AeroDrop configuration is a lift-modulated orbiter with a ballistic probe trajectory. The ballistic probe trajectory could be truly passive, such as for a simple penetrator probe mission, or it could apply drag-modulation to the ballistic trajectory for the purpose of accommodating uncertainties. Passive impact or penetrator probes are already excellent candidates for AeroDrop due to their simplicity and small size, so this architecture stands out as a promising version of AeroDrop for multiple reasons.

CONCLUSION

AeroDrop is a promising architecture that enables new kinds of smallsat ride-along missions to interplanetary destinations. By sharing target entry conditions with the primary probe or orbiter, these secondary missions maximize their benefit from the primary while minimizing their impact on the primary mission. The possibility of AeroDrop is demonstrated for Earth, Mars, Venus, Titan, and Neptune, and the high-level regions of feasibility are characterized. Passive impact or penetrator probes on a ballistic nominal trajectory as the secondary mission on an orbiter delivered by a lift-modulated nominal aerocapture trajectory are shown to be the most promising AeroDrop configuration. A number of challenges remain for AeroDrop implementation, including separation design, timing and observation geometry, packaging, and tight volume and mass constraints.

ACKNOWLEDGMENT

This work was supported by a NASA Space Technology Research Fellowship.

REFERENCES

[1] "Smallsats by the Numbers 2020," tech. rep., Bryce Space and Technology, 2020.

[2] A. Poghosyan and A. Golkar, "CubeSat evolution: Analyzing CubeSat capabilities for conducting science missions," *Progress in Aerospace Sciences*, Vol. 88, January 2017, pp. 59–83.

[3] C. D. Norton, S. Pellegrino, and M. Johnson, "Small Satellites: A Revolution in Space Science," tech. rep., Keck Institute for Space Studies, California Institute of Technology, July 2014.

[4] T. Talbert, "NASA Selects CubeSat, SmallSat Mission Concept Studies," 2017. accessed 05-21-2020.

[5] S. W. Asmar and S. Matousek, *Mars Cube One (MarCO): Shifting the Paradigm in Relay Deep Space Operation*, ch. OCFE - Mission Ops Concept I, pp. 1–7. American Institute of Aeronautics and Astronautics, 2016.

[6] M. I. Cruz, "The aerocapture vehicle mission design concept," *Conference on Advanced Technology for Future Space Systems*, AIAA, May 1979, 10.2514/6.1979-893.

[7] H. S. Wright, D. Y. Oh, C. H. Westhelle, J. L. Fisher, R. E. Dyke, K. T. Edquist, J. L. Brown, H. L. Justh, and M. M. Munk, "Mars Aerocapture Systems Study," Tech. Rep. TM-2006-214522, NASA, 2006.

[8] P. Gage, M. Mahzari, K. Peterson, D. Ellerby, and E. Venkatapathy, "Technology Readiness Assessment for HEEET TPS," *16th International Planetary Probe Workshop*, July 2019.

[9] Z. R. Putnam and R. D. Braun, "Drag-Modulation Flight-Control System Options for Planetary Aerocapture," *Journal of Spacecraft and Rockets*, Vol. 51, No. 1, 2014, pp. 139–150, 10.2514/1.A32589.

[10] T. R. Spilker, M. Adler, N. Arora, P. M. Beauchamp, J. A. Cutts, M. M. Munk, R. W. Powell, R. D. Braun, and P. F. Wercinski, "Qualitative Assessment of Aerocapture and Applications to Future Missions," *Journal of Spacecraft and Rockets*, Vol. 56, Mar.-Apr. 2019, pp. 536–545.

[11] M. Hofstadter, A. Simon, K. Reh, J. Elliott, C. Niebur, and L. Colangeli, "Ice Giants Pre-Decadal Study Final Report," tech. rep., NASA, June 2017.

[12] J. L. Hall, A. N. Noca, and R. W. Bailey, "Cost-Benefit Analysis of the Aerocapture Mission Set," *Journal of Spacecraft and Rockets*, Vol. 42, No. 2, 2005, pp. 309–320.

[13] S. W. Albert and R. D. Braun, "Conceptual Development of AeroDrop: Aerocapture and Direct Entry for Two Spacecraft on a Common Approach Trajectory," *AIAA Scitech 2020 Forum*, AIAA, 2020, 10.2514/6.2020-1737.

[14] "Viking Mission to Mars - NASA Fact Sheet," https://mars.nasa.gov/internal_resources/828/.

[15] "Viking 1 Lander - NASA Space Science Data Coordinated Archive," https://nssdc.gsfc.nasa.gov/nmc/spacecraft/display.action?id=1975-075C.

[16] R. D. Braun and R. M. Manning, "Mars Exploration Entry, Descent, and Landing Challenges," *Journal of Spacecraft and Rockets*, Vol. 44, No. 2, 2007.

[17] W. J. O'Neil, *The Three Galileos: The Man, the Spacecraft, the Telescope*, Vol. 220, ch. The Galileo Spacecraft Architecture. Springer, Dordrecht, 1997.

[18] B. Kazeminejad, D. H. Atkinson, M. Pérez-Ayúcar, J.-P. Lebreton, and C. Sollazzo, "Huygens' entry and descent through Titan's atmosphere—Methodology and results of the trajectory reconstruction," *Planetary and Space Science*, Vol. 55, No. 13, 2007, pp. 1845 – 1876. Titan as seen from Huygens, https://doi.org/10.1016/j.pss.2007.04.013.

[19] A. J. Ball, J. R. C. Garry, R. D. Lorenz, and V. V. Kerzhanovich, *Planetary Landers and Entry Probes*. Cambridge University Press, 2009.

[20] T. J. Martin-Mur, G. L. Kruizingas, P. D. Burkhart, M. C. Wong, and F. Abilleira, "Mars Science Laboratory Navigation Results," *23rd International Symposium on Space Flight Dynamics*, Jet Propulsion Lab., California Inst. of Tech., 2012.

[21] "Mars 96 Orbiter - NASA Space Science Data Coordinated Archive," https://nssdc.gsfc.nasa.gov/nmc/spacecraft/display.action?id=1996-064A.

[22] "THOR – Tracing Habitability, Organics, and Resources," http://thor.asu.edu/overview/index.html, 2007.

[23] H. S. Wright, M. A. Croom, R. D. Braun, G. D. Qualls, P. Cosgrove, and J. S. Levine, "ARES Mission Overview - Capabilities and Requirements of the Robotic Aerial Platform," *2nd AIAA "Unmanned Unlimited" Conf. and Workshop & Exhibit*, 2003, 10.2514/6.2003-6577.

[24] A. T. Klesh, J. Baker, and J. Krajewski, "MarCO: Flight Review and Lessons Learned," *Small Satellite Conference*, 2019.

[25] R. Hodges, N. Chahat, D. Hoppe, and J. Vacchione, "A Deployable High-Gain Antenna Bound for Mars: Developing a new folded-panel reflectarray for the first CubeSat mission to Mars.," *IEEE Antennas and Propagation Magazine*, Vol. PP, 02 2017, pp. 1–1, 10.1109/MAP.2017.2655561.

[26] M. S. Werner and R. D. Braun, "Mission Design and Performance Analysis of a Smallsat Aerocapture Flight Test," *Journal of Spacecraft and Rockets*, Vol. 56, No. 6, 2019, pp. 1704–1713, 10.2514/1.A33997.

[27] A. Austin, A. Nelessen, B. Strauss, J. Ravich, M. Jesick, E. Venkatapathy, R. Beck, P. Wercinski, M. Aftosmis, M. Wilder, G. Allen, R. Braun, M. Werner, and E. Roelke, "SmallSat Aerocapture to Enable a New Paradigm of Planetary Missions," *2019 IEEE Aerospace Conference*, 2019, pp. 1–20.

[28] K. Sutton and R. A. Graves, "A General Stagnation-Point Convective-Heating Equation for Arbitrary Gas Mixtures," Tech. Rep. TR R-376, NASA, 1971.

[29] "Mars Fact Sheet - NASA Space Science Data Coordinated Archive," https://nssdc.gsfc.nasa.gov/planetary/factsheet/marsfact.html.

[30] "Venus Fact Sheet - NASA Space Science Data Coordinated Archive," https://nssdc.gsfc.nasa.gov/planetary/factsheet/venusfact.html.

[31] C. G. Justus and R. D. Braun, "Atmospheric Environments for Entry, Descent and Landing (EDL)," *5th International Planetary Probes Workshop and Short Course*, 2007.

[32] "Neptune Fact Sheet - NASA Space Science Data Coordinated Archive," https://nssdc.gsfc.nasa.gov/planetary/factsheet/neptunefact.html.

[33] J. D. Anderson, *Hypersonic and High-Temperature Gas Dynamcis*, ch. Chapter 3: Local Surface Inclination Methods and Chapter 6: Viscous Flow: Basic Aspects, Boundary Layer Results, and Aerodynamic Heating, p. 55 and 347. AIAA.

[34] D. Prabhu and D. Saunders, "On Heatshield Shapes for Mars Entry Capsules," *50th AIAA Aerospace Sciences Meeting including the New Horizons Forum and Aerospace Exposition*, AIAA, 2012, 10.2514/6.2012-399.

[35] D. Way, R. Powell, A. Chen, A. Steltzner, M. San Martin, P. Burkhart, and G. Mendeck, "Mars Science Laboratory: Entry, Descent, and Landing System Performance," *IEEE Aerospace Conference Proceedings*, March 2006.